Anti Crystallization Blocking of Flocking Drainage Pipe Based on Natural Phenomenon

Xuefu ZHANG [1, 2], Shiyang LIU [1, 2] *, Feng GAO [1, 2], Yuanfu ZHOU [1, 2], Bin ZHANG [1]

[1] *State Key Laboratory of Mountain Bridge and Tunnel Engineering, Chongqing Jiaotong University, Chongqing 400074, China*
[2] *College of Civil Engineering, Chongqing Jiaotong University, Chongqing 400074, China*

crossref http://dx.doi.org/10.5755/j02.ms.29891

Received 05 October 2021; accepted 02 March 2022

Crystalline pipe plugging of the tunnel drainage system was one of the causes of tunnel lining cracking and water leakage. Effective prevention of crystalline pipe plugging of tunnel drainage pipe was very important to ensure the safety and stability of lining structure during tunnel operation. Using the methods of field investigation, indoor model test and numerical simulation, a new flocking anti crystallization blocking technology was proposed. The crystallization law and anti-crystallization efficiency of the flocked drainage pipe at different flow rates, the three-dimensional flow field distribution characteristics and the crystal distribution law of flocking drainage pipe were studied. The results show that the maximum crystallization rate of nonflocked drainage pipe was 1.30 g/d. The maximum stable attachment amount of crystals in flocked drainage pipe was 18.13 g, and the maximum anti crystallization efficiency can reach 80 %. The flocked drainage pipe can preferentially select the villus with the length of 5 mm and 10 mm. The flow velocity at the top of flocked drainage pipe increased by 35 %. Crystals near the water inlet of flocked drainage pipe were mainly distributed on both sides, near the water outlet were mainly distributed in the middle and lower part of the drainage pipe, and were attached to the wall surface of the drainage pipe at the water outlet. Flocked parameters of flocked drainage pipe (flocking material, flocking length, flocking diameter, flocking longitudinal spacing and flocking circumferential spacing, etc.) also need a lot of experimental research, so that the research results can truly solve the practical engineering problems.
Keywords: tunnel, pipe plugging by crystallization, flocking drainage pipe, three-dimensional flow field, crystal distribution.

1. INTRODUCTION

By the end of 2019, 19067 highway tunnels were operating on the Chinese mainland, including 1175 super long tunnels and 4784 long tunnels. In the process of tunnel operation, various types of problems gradually appear, including lining leakage (Fig. 1) and lining cracking (Fig. 2) caused by crystal plugging of the tunnel drainage system (Fig. 3) in karst areas.

Fig. 1. Water box at a leak in the lining

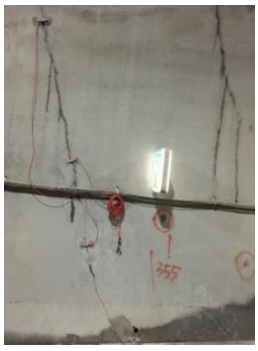

Fig. 2. Cracked lining

At present, in light of the problem of crystal plugging of tunnel drainage systems, only high-pressure gas (water) or excavation can be used for dredging, both of which are expensive and seriously affect the normal operation of a tunnel [1].

Fig. 3. Crystal blockage of a drainage pipe

To consider the problem of crystal clogging of tunnel drainage systems, this study focused on crystal composition analysis, analysis of the factors influencing the crystals, and crystal prevention and treatment techniques. The main component of the crystals in tunnel drainage pipes is insoluble calcium carbonate [2 – 4], and the calcium in the crystals comes mainly from the underground water [2, 5] and the cement in the shotcrete [6]. The main factors influencing crystallization plugging include the CO_2 partial pressure, flow rate, temperature, pH value, ion species, and concentration [7, 8]. The amount of crystallization in the drainage pipe increases with increasing pH value, and the

* Corresponding author. Tel.: +023-62789147; fax: +023-62650561.
E-mail address: *liushiyang@mails.cqjtu.edu.cn* (S. Liu)

calcium carbonate crystals are spindle shaped. The larger the pH value is, the smaller the grain size is, the more uniform the grain size is, and the more compact the accumulation [9]. Hydrophobic treatment of the concrete base and the polyvinyl chloride (PVC) pipe wall with a protective coating can reduce the adhesion of calcium carbonate crystals [10, 11]. By optimizing the concrete materials and the proportions of the mixtures, reducing the contact between the groundwater and concrete, preventing CO_2 from entering the tunnel drainage pipe, adding appropriate amounts of fly ash to the shotcrete, and taking other measures, the formation of crystals can be effectively reduced [8, 12]. The crystals in drainage pipes are mainly insoluble calcite, and the phase transition from aragonite to calcite can be prevented by triblock copolymers (PEG-b-PAA-b-PS, poly (ethylene glycol)-block-poly (acrylic acid)-block-poly(styrene)) [13]. In the presence of biopolymers, the relative vaterite content increases with the application of ultrasonic treatment [14]. The ultrasonic treatment makes the aggregated calcium carbonate crystals more brittle [15]. With the increase of ultrasonic frequency, the net fouling deposition rate increases and the fouling thermal resistance increases [16]. Electromagnetic treatment reduces the theoretical adhesion work and reduces the adhesion ability of calcium carbonate particles on the surface of small rust steel [17]. The magnetic shielding effect is reduced, and the descaling, anti-scaling and corrosion inhibition effects of the electronic descaling instrument are improved [18]. Electroless Ni-W-P coating with low surface free energy reduces the fouling deposition rate by 52 % [19]; The surface of ternary Ni-Cu-P coating can significantly inhibit the adhesion of dirt [20]; Amorphous Ni-Mo-P alloy coating has good scale inhibition ability [21].

The crystal structure of the calcium carbonate is changed from calcite to aragonite by green corrosion inhibitor RS1600 [22]. The cleaning solvents of single-molecule carboxylic acid organic acid reagent and polymeric carboxylic acid organic acid reagent with concentrations of 2000 ppm and dichromate indexes of 17.71 % can effectively remove karst crystals from drainage systems on the premise of ensuring green environmental protection [23].

These studies have promoted research on the crystal blockage problem in tunnel drainage systems. After the completion of the tunnel, the entire drainage system is a closed system. Before the implementation of these treatment measures, we need to accurately find the specific location of the drainage pipe and then open the drainage pipe in a destructive manner, which undoubtedly increases the maintenance cost of the tunnel. Therefore, based on the natural phenomenon (raindrops on the cable in rainy days will not increase with the growth of rain time and will fall off when raindrops increase to a certain extent; Fig. 4), starting from the structure of the drainage pipe, we proposed a flocking drainage pipe anti-crystal-plugging technique. The technique used the characteristics of the drainage pipe to prevent the occurrence of the crystallization plugging phenomenon.

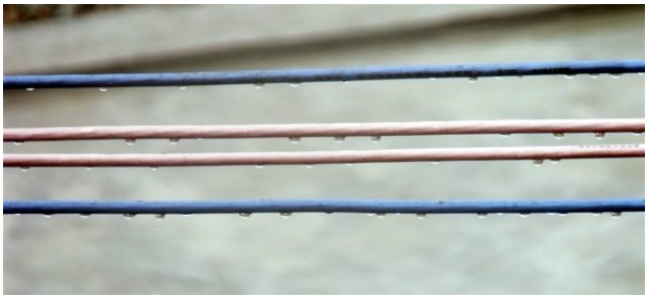

Fig. 4. Raindrops on cables on a rainy day

Based on the natural phenomenon, in this paper, an anti-crystal-plugging technique for tunnel flocked drainage pipes is proposed. Through field investigations and indoor data query, a 1:1 indoor model testing device was designed to study the anticrystallization efficiency of four types of pile length of flocked drainage pipes under three flow velocities, and the ANSYS Fluent software was used to analyze the three-dimensional flow field distribution characteristics and the crystal distribution in the flocking drainage pipe.

2. METHODS

2.1. Laboratory model tests

Through on-site investigations and data access, we obtained basic geometric parameters, such as the diameter of the transverse drainage pipe, the slope of the drainage pipe, and the length of the drainage pipe, and determined the geometric similarity parameters of the indoor model testing device (Table 1). Through field tests of the groundwater velocity in the crystallization area in the tunnel drainage pipe, we determined the motion similarity parameters of the indoor testing model device (Fig. 5) and the temperature and humidity of the model test environment. Combined with the similarity theory of the model test, we designed a 1:1 indoor model testing device to provide a reliable test platform for the indoor testing of flocking drainage pipes (Fig. 6). Three test flow rates were used [24]. The main cation in the test solution was calcium ion, the main anion was bicarbonate, and the CO_3^{2-} mainly came from the CO_2 dissolved in the testing solution [2, 5]. As shown in Fig. 7.

Table 1. Main parameters of the model testing device

Project	Parameter	Project	Parameter
Diameter of flocked drainage pipe	100 mm	Sectional shape of flocked drainage pipe	Semicircle
Slope of flocked drainage pipe	3 %	Testing solution	Calcium bicarbonate saturated solution
Length of flocked drainage pipe	1500 mm	Villus length	5 mm, 10 mm, 15 mm, 20 mm
Villus diameter	0.6 mm	Longitudinal distance of villus	25 mm
Circumferential distance of villus	10°	Velocity	2.91 cm/s, 5.46 cm/s, 8.20 cm/s [24]

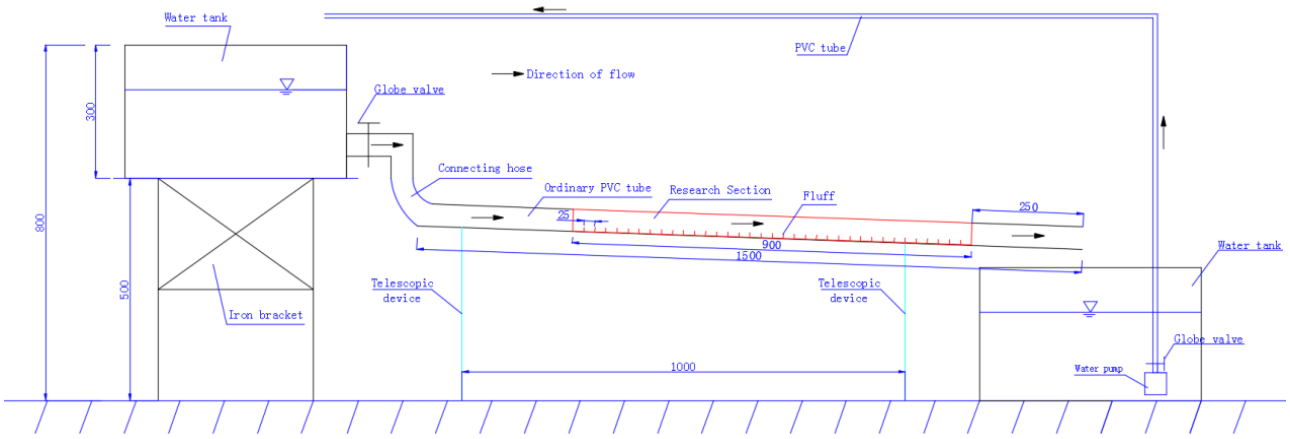

Fig. 5. Indoor model testing facility 1:1 (unit: mm)

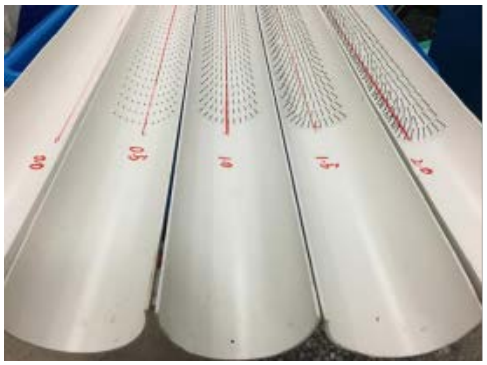

Fig. 6. Flocking drain pipe

Through the 1:1 indoor model testing device, we analyzed the change rule of the number of crystals and the efficiency of preventing crystal blockage of a flocked drainage pipe under three flow rates and analyzed the macroscopic distribution rule and microscopic morphology of the crystals. The longest culture time for the types of calcium carbonate crystals was no more than 144 hours [25]. It can be inferred that when the test period is longer than 144 hours (i.e., 6 days), crystals with significant crystal morphology will appear. It is reasonable to take 10 days (9 days of operation and 1 day off standing) as a test tube weighing cycle. The indoor model tests run are shown in Fig. 7.

Fig. 7. Indoor model testing operation

We allowed the test pipe to stand at room temperature (average temperature of 22.5°C and average humidity of 80.8%) for 1 day and weighed the drainage pipe using an electronic scale with an accuracy of 0.01 g (Fig. 8). We calculated the weight of the crystals in the testing drainage pipe according to Eq. 1:

$$m = M_i - M_0 \quad (1)$$

where m is the weight of the crystals in the test drainage pipe every i days; i is the weighing interval of 10 days, 20 days, 30 days, 40 days, and 50 days; M_i is the weight of the test drain on the day i; and M_0 is the initial weight of the test drain.

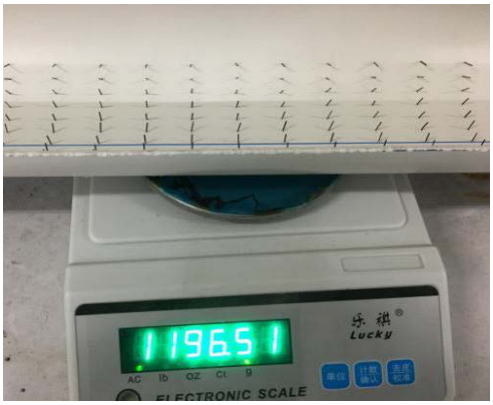

Fig. 8. Weighing the test drain pipe

2.2. Numerical simulation

The higher the velocity of the water in the drainage pipe, the lower the amount of crystallization [24]. We analyzed the flow field distribution characteristics of flocked drainage pipe and common drainage pipe using the FLUENT software. By using the multiphase (volume fluid) model of the fluent chemical reaction module and the specifications (transport specifications) model of component transport, we analyzed the crystal distribution characteristics during water flow in the flocked drainage pipe using the ion concentration of the testing solution. The main parameters of the numerical calculation model were as follows: the flow rate was 2.0 cm/s, the diameter of the pile was 0.6 mm, the length of the pile was 20 mm, the longitudinal spacing of the pile was 25 mm, and the circumferential spacing of the pile was 10°. The calculation model is illustrated in Fig. 9, in which the groundwater flows along the Z direction. Table 2 shows the analysis conditions of the flow field and crystal distribution of flocking drainage pipe.

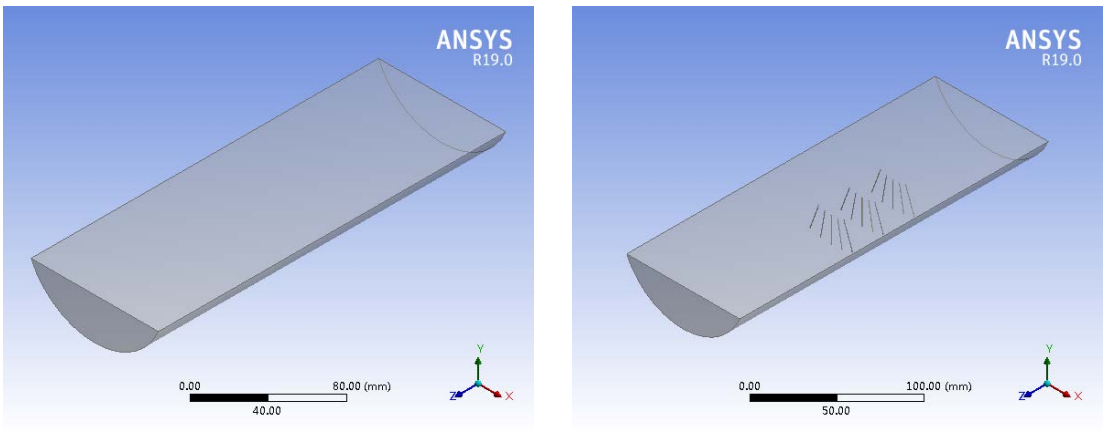

a b

Fig. 9. Geometric model: a – nonflocked drainage pipe; b – flocked drainage pipe

Table 2. Geometric positions and analysis conditions

Analysis of working conditions	Position	Analysis of working conditions	Position
Flow field and crystal distribution	X = 0	Velocity	y = 3 mm
	Z = 0.05 m (nonflocked)		y = 8 mm
	Z = 0.08 m (flocked)		y = 13 mm
	Z = 0.105 m (flocked)		y = 18 mm
	Z = 0.13 m (flocked)		y = 23 mm
	Z = 0.15 m (nonflocked)		/

3. RESULTS AND DISCUSSION

3.1. Laboratory model tests

In Fig. 10, Fig. 11 and Fig. 12, the legend value of 0 represents the non-flocked drainage pipe, and the legend value of 5, 10, 15, and 20 represents the flocked drainage pipe.

Fig. 10 shows the change in the amount of crystallization in the test drainage pipe with time for a flow rate of 2.91 cm/s. The crystallization rate of the unplanted drainage pipe was 1.30 g/d, which was consistent with that of Liu et al. [24].

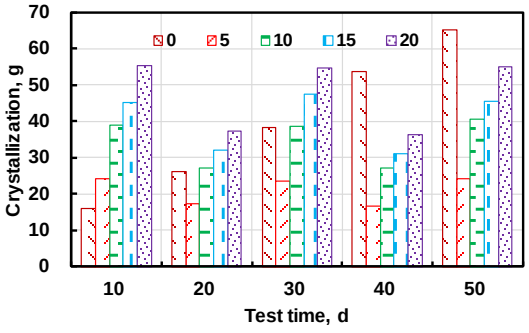

Fig. 10. Variation in the crystallization in the flocked drainage pipe with time (2.91 cm/s)

At the same time, the crystallization change law of drainage pipe when the groundwater temperature was 30 – 40 °C studied by Feng et al. [26] was verified. The change in the crystallinity of the flocked drainpipes was W-shaped, and it increased with increasing pile length. When the pile length was 5 mm, the stable crystallization (the difference between the peak and valley crystallization) in the flocking drainage pipe was 7 g; when the pile length was 10 mm, the stable crystallization was 11.88 g; when the pile length was 15 mm, the stable crystallization was 13.24 g; and when the pile length was 20 mm, the stable crystallization was 18.13 g. As can be seen, the pile length was directly proportional to the amount of crystal attachment. At the beginning of the experiment (10 days), the crystallization in the flocked drainage pipes was greater than that in the nonflocked drainage pipes. After 20 days, the crystallization in the flocked drainage pipes decreased. The crystallization in the 5 mm pile length drainage pipe was less than that in the nonflocked drainage pipes. The crystallization in the 10 mm pile length drainage pipe was close to that in the nonflocked drainage pipes. The crystallization in the 15 mm and 20 mm pile length drainage pipes was still large for the nonflocked drainage pipes. After 30 days, the crystallization in the fluff drainage pipe increased again. The crystallization in the 10 mm long fluffed drainage pipe was close to that in the nonfluffed drainage pipe. The crystallization in the 15 mm and 20 mm long fluffed drainage pipes was still greater than that in the nonfluffed drainage pipes. After 40 days, the amount of crystallization in the nonflocked drainage pipe was greater than that in the flocked drainage pipe. At the end of the test, the amount of crystallization in the nonflocked drainage pipe was the greatest and that in the flocked drainage pipe with a 5 mm pile length was the least.

Fig. 11 shows the change in the amount of crystallization in the test drainage pipe with time for a flow rate of 5.46 cm/s. The crystallization rate in the nonflocked drainage pipe was 0.891 g/d, which was less than the flow rate of 2.91 cm/s. During the entire experiment, the crystallization in the 5 mm pile drainage pipe was less than that in the nonpile drainage pipe.

As the pile length increased, the crystallization in the flocked drainpipe gradually increased.

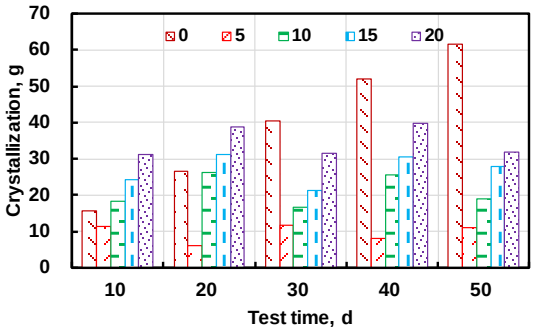

Fig. 11. Variation in the crystallization in the flocked drainage pipe with time (5.46 cm/s)

The results showed that the stable crystallization in the 5 mm, 10 mm, 15 mm, and 20 mm length drainage pipes was 4.31 g, 6.61 g, 7.15 g, and 7.87 g, respectively. The fluff length was approximately proportional to the amount of crystal attachment. As the flow rate increased, the stable crystallization in the drainage pipes decreased. The experimental results verified the research conclusions of Liu et al. [27]. In the initial stage of the experiment (10 days), the crystallization in the 5 mm pile drainage pipe was less than that in the nonpile drainage pipe; and the crystallization in the other pile drainage pipes was greater than that in the nonpile drainage pipe. The crystallization in the 20 mm pile drainage pipe was the greatest. At the end of the experiment, the crystallization in the nonflocked drainage pipe was the greatest and that in the 5 mm flocked drainage pipe was the least.

Fig. 12 shows the change in the amount of crystallization in the test drainage pipe with time for a flow rate of 8.20 cm/s.

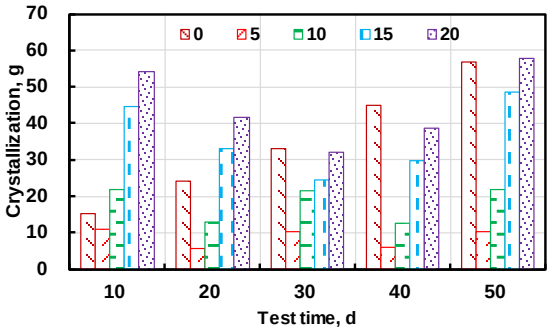

Fig. 12. Variation in crystallization in the flocked drainage pipe with time (8.20 cm/s)

The crystallization rate was 1.218 g/d. During the entire experiment, the crystallization in the drainage pipe with a 5 mm pile length was less than that in the drainage pipe without a pile length. After 20 days, the crystallization in the flocked drainpipes was less than that in the nonflocked drainpipes. The stable crystallization in the flocked drainpipes with 5 mm and 10 mm villus lengths was 5.29 g and 9.26 g, respectively. The results showed that the change in the crystallization in the flocked drainage pipes with 15 mm and 20 mm villus lengths was V-shaped. The crystallization was the greatest at the beginning and end of the experiment, and the least in the middle of the experiment (30 days).

From the analysis of the crystallization of each flocked drainage pipe under the above three flow rates, it can be seen that the variation law of the crystallization of flocked drainage pipe with the test time was similar to the natural phenomenon mentioned in the introduction, and there were differences in the crystallization of flocked drainage pipe under the condition of each length of the villus. This was mainly because the flow rate of groundwater in the drainage pipe and the length of the villus had a certain impact on the adhesion of crystallization. When the flow velocity of groundwater and villus length in the pipe were different, the times of contact between cation and anion in groundwater were also different, resulting in large dispersion of crystallization. The follow-up test can prolong the test operation cycle and increase the weighing cycle to find the highest and lowest peaks of crystallization.

The anticrystallization efficiency of the indoor test drainage pipe was calculated using Eq. 2. The relationship between the anticrystallization efficiency of the flocked drainage pipe and the pile length under three flow rates is shown in Fig. 13.

$$\eta = \frac{M_n - M_z}{M_n} \times 100, \tag{2}$$

where M_n is the total amount of crystallization in the nonflocked drainage pipe; and M_z is the total amount of crystallization in the flocked drainage pipe.

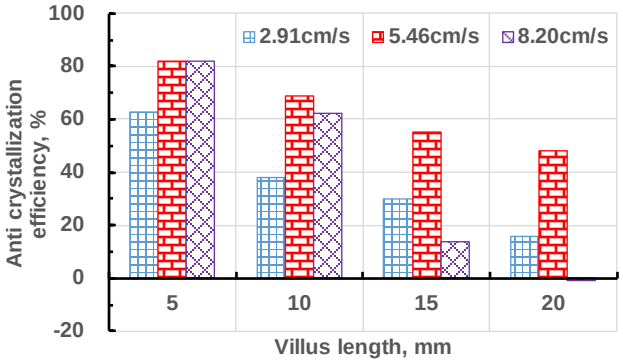

Fig. 13. Anticrystallization efficiency of the flocked drainage pipes with different pile lengths

Under the three flow rates, the anticrystallization efficiency decreased with increasing villus length. When the flow rate was 2.91 cm/s, the anticrystallization efficiency was 20 – 60 %; when the flow rate was 5.46 cm/s, the anticrystallization efficiency was 50 – 80 %; and when the flow rate was 8.20 cm/s, the anticrystallization efficiency was 0 – 80 %. Under the high flow rate, only the flocked drainage pipes with 5 mm and 10 mm fluff lengths exhibited better anticrystallization efficiencies. Under the low and medium flow rates, the flocked drainage pipes with various pile lengths exhibited better anticrystallization efficiencies. In general, the anticrystallization efficiencies of the 5 mm and 10 mm fluff length flocked drainage pipes reached more than 40 % at each flow rate, which can be used in the field test of the anticrystallization plugging of flocked drainage pipes.

3.2 Numerical simulation analysis

Fig. 14 shows the three-dimensional flow fields in the nonflocked drainage pipe and the flocked drainage pipe at different cross-section positions. The maximum velocity in the nonflocked drainage pipe was 2.98 cm/s and that in the flocked drainage pipe was 3.06 cm/s, which was 2.68 higher than that in the nonflocked drainage pipe. The distribution of the flow field in the nonflocked drainage pipe was regular and gradually increased from the outside to the inside.

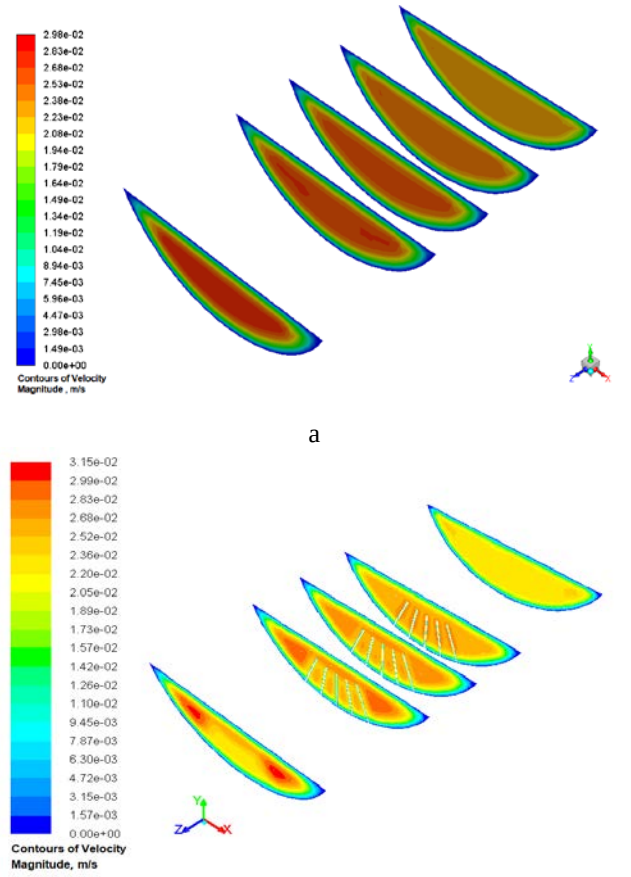

Fig. 14. Cross-section cloud of the three dimensional flow fields in the test drainage pipes: a – nonflocked drainage pipe; b – flocked drainage pipe

The local distribution of the flow field in the flocked drainage pipe was relatively disordered, and the maximum flow velocity was distributed on both sides of the nonflocked drainage pipe. In section z = 0.050 m, the velocity distribution in the middle of the nonflocked drainage pipe was regular, the flow field formed a closed area, and high velocity areas were formed on both sides of the flocked drainage pipe. In section z = 0.080 m, the velocity distribution in the middle of the nonflocked drainage pipe was still relatively regular, and the velocity increased. In the flocked drainage pipe, it formed an arc-shaped region with a higher velocity in the range of the pile height and gradually extended to both sides. In section z = 0.105 m, the velocity distribution in the middle of the nonflocked drainage pipe was still regular, the velocity on both sides of the flocked drainage pipe increased, and the velocity in the rest was the same as that in section z = 0.080 m. In section z = 0.130 m, there were areas with large velocities above and on both sides of the pile. In section z = 0.180 m, the maximum velocity was distributed in the upper part of the flocked drainage pipe section, which is approximately a straight line. The velocity stratification in the nonflocked drainage pipe section was obvious, forming a closed drainage basin.

Fig. 15 shows the flow field nephogram of the nonflocked and flocked drainage pipes in section x = 0. The results showed that the distribution of the flow field in the nonflocked drainage pipe was regular, and the flow velocity increased gradually along the direction of the flow velocity.

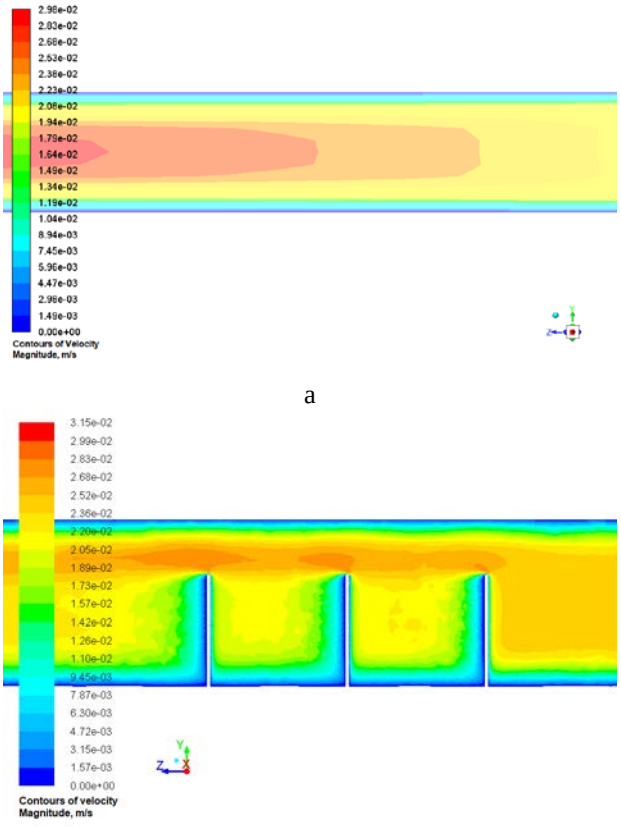

Fig. 15. Comparison of the flow field nephograms of the x = 0 sections of the flocked and nonflocked drainage pipes: a – nonflocked drainage pipe; b – flocked drainage pipe

There were more low-flow velocity areas in the front and back of the fluffed section and between the fluff in the flocked drainage pipe than in the nonflocked drainage pipe, but there were more high-flow velocity areas than in the nonflocked drainage pipe.

Fig. 16 shows the velocity distribution curve at five monitoring positions along the longitudinal direction. When y = 3 mm, the velocity in the nonflocked drainage pipe gradually decreased along the longitudinal direction. Finally, it approached 1.4 cm/s, and the velocity decreased by 30 %. The velocity in the flocked drainage pipe also gradually decreased along the longitudinal direction, forming a velocity ladder between the villi. Finally, it approached 1.25 cm/s, and the velocity decreased by 37.5 %. The velocity in the drainage pipe without flocking at y = 8 mm increased along the longitudinal direction. The velocity was close to 2.6 cm/s and increased by 30 %. The velocity in the drainage pipe with flocking increased along

the longitudinal direction, increased to 2.5 cm/s in the first row (z = 0.08 m) of fluff, decreased to 2.2 cm/s after the fluff, and increased to 2.5 cm/s (by 25 %).

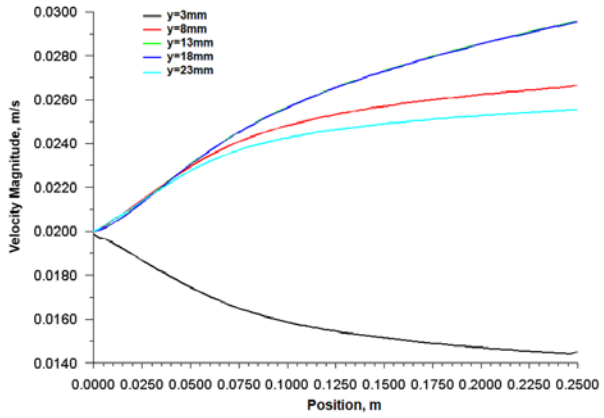

a

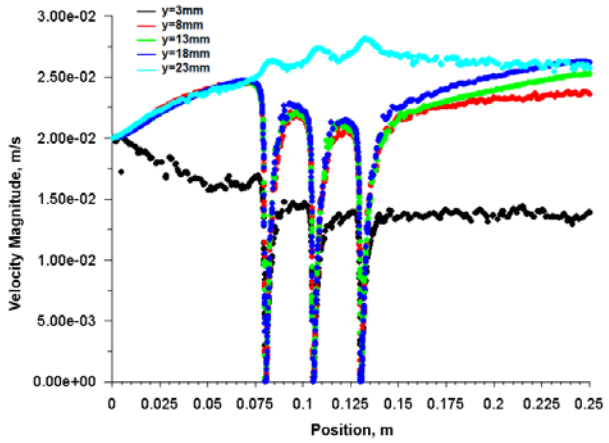

b

Fig. 16. Comparison of the longitudinal velocity at five monitoring positions in section x = 0 in the flocked and nonflocked drainage pipes: a – nonflocked drainage pipe; b – flocked drainage pipe

The changes in velocity in the nonflocked drainage pipe at y = 13 mm and y = 18 mm were the same, that is, gradually increasing along the longitudinal direction and finally approaching 3.0 cm/s. The velocity increased by 50 %. The velocity in the flocked drainage pipe at y = 13 mm gradually increased to 2.75 cm/s, whereas at y = 18 mm, it gradually increased to 3.2 cm/s, that is, the velocity increased by 37.5 % and 60 %, respectively. When y = 23 mm, the flow velocity in the nonflocked drainage pipe increased gradually along the longitudinal direction. Finally, it approached 2.5 cm/s (i.e., by 25 %). The flow velocity in the flocked drainage pipe increased gradually along the longitudinal direction to 2.7 cm/s (i.e., by 35 %). Fig. 17 shows the distribution of the crystals in section x = 0 in the flocked drainage pipe. The maximum crystal content in the flocked drainage pipe was 2.03×10^{-7}. Along the direction of the groundwater flow in the drainage pipe, the crystals gradually transitioned from the upper part of the drainage pipe to the bottom of the drainage pipe, and more crystals accumulated in the front and back of the lower part of the pile.

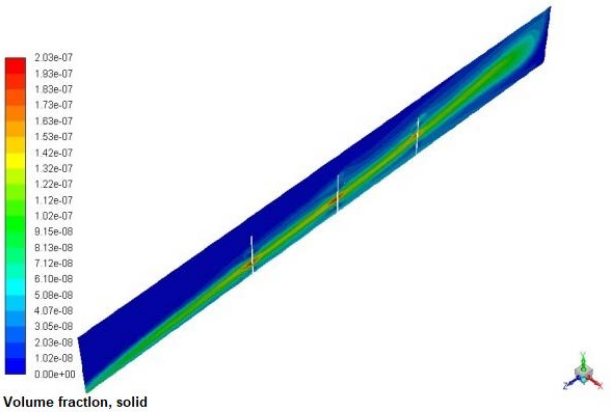

Fig. 17. Crystal distribution in section x = 0 in the flocking drainage pipe

For the flocked drainage pipes, the crystals near the water inlet were distributed mainly in the middle and upper parts of the pile, while the crystals near the water outlet were distributed mainly in the middle and lower parts of the pile, and the crystals gradually were deposited along the flow direction of the drainage pipe.

Fig. 18 shows the distribution of crystal in each section of the flocked drainage pipe. The crystal mass fraction of the flocked drainage pipe in section z = 0.050 m was 7.75×10^{-7}, and the crystals were distributed on both sides of the drainage pipe. The crystals were mainly suspended in the underground water in the drainage pipe and fewer crystals appeared in the center above the bottom of the drainage pipe. The maximum mass fraction of crystals was 5.17×10^{-7} in section z = 0.08 m.

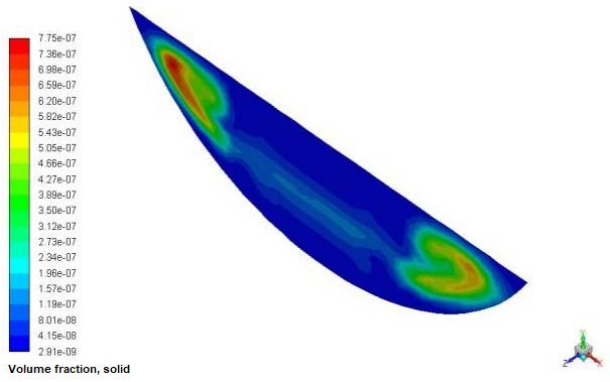

a

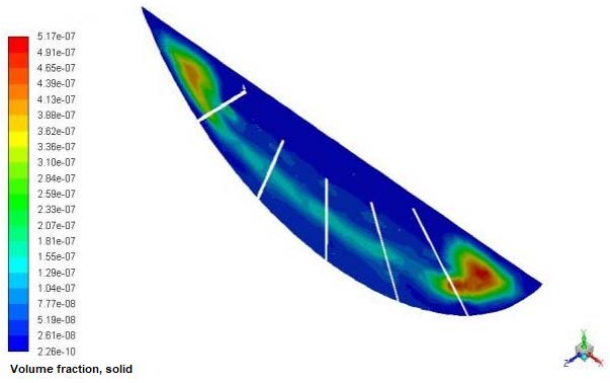

b

continued on next page
continuation

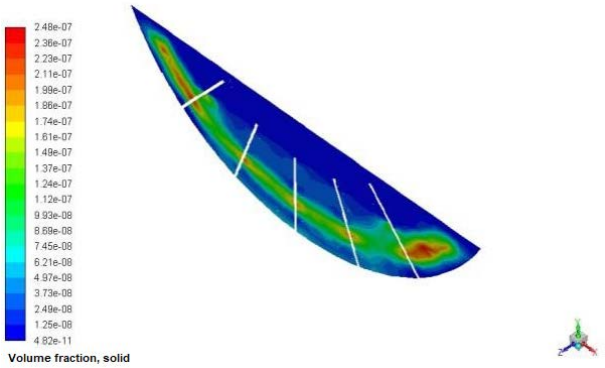

c

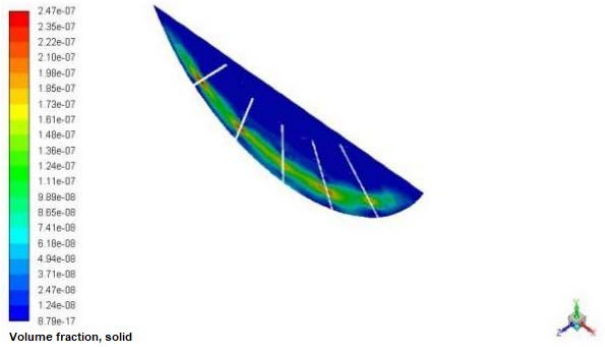

d

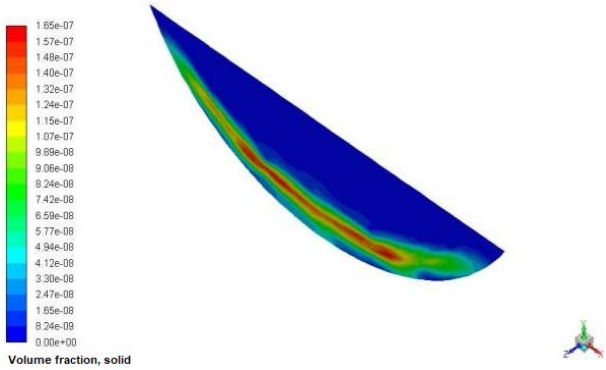

e

Fig. 18. Crystal distribution in cross sections of the flocked drainage pipe: a – Z = 0.050 m; b – Z = 0.080 m; c – Z = 0.105 m; d – Z = 0.130 m; e – Z = 0.180 m

With the water flow in the drainage pipe, the crystals gradually transferred from both sides to the middle and upper parts and fewer crystals appeared near the pile. The crystal mass fraction in the flocked drainage pipe in section z = 0.105 m was 2.48×10^{-7}, and the crystals gradually accumulated near the middle of the pile, especially in the lower part of the pile. The crystal mass fraction in the flocked drainage pipe in section z = 0.130 m was 2.47×10^{-7}. The crystals were distributed mainly in the lower part of the pile and the underground water suspended between the piles, and the number of crystals on both sides gradually decreased. The crystal mass fraction in the flocked drainage pipe in section z = 0.180 m was 1.65×10^{-7}, the crystals gradually accumulated in the middle and lower parts of the drainage pipe. The crystals gradually sank near the bottom surface of the drainage pipe, and they finally adhered to the surface of the drainage pipe. The numerical simulation shows that the tunnel drainage pipe is easy to form crystals near the water outlet, and further deposits into the pipe to block the drainage pipe, which was consistent with the field investigation [7, 12].

It can be seen from Fig. 19:

1. Under the condition of low flow rate, the water level in the cross section of the drainage pipe was low (less than 10 mm), there was no crystallization on 1 – 2 rows of villus on both sides of the flocked drainage pipe wall, or only a small part, but there was a large amount of crystallization on 3 – 5 rows of a villus in the middle of the bottom and both sides of the drainage pipe.
2. Crystals were distributed along the length of the villus and wrapped the villus. Along the water flow direction, there were fewer crystals between the transverse villus and more crystals between the longitudinal villus, especially before and after the position of the villus.
3. The the villus were short and almost wrapped by crystals along the length of villus; when the villus was long, only the length below and above the water line was wrapped with crystals.

Fig. 19. Crystal distribution of flocked drainage pipe when the villus length was 20 mm (2.91 cm/s)

The distribution law of crystals in the laboratory test was similar to the numerical simulation results. More crystals were distributed near the pipe wall of the villus. The closer it was to the water outlet, the more crystals were in the lower part of the villus. In the subsequent numerical simulation process, the concentration of anion and cation in groundwater can be increased and the numerical simulation time can be prolonged, so that the calculation results can be compared with the indoor test more accurately.

3.3. Comparative analysis of the use of flocking drainage pipes to prevent crystal blockage

The results of the laboratory tests revealed that the amount of crystallization in the nonflocked drainage pipe increased linearly with time, which was consistent with the results of Liu et al. [24]. The test results showed that the anticrystallization efficiency of the 5 mm and 10 mm pile length drainage pipes reached more than 40 % at each flow rate, and the anticrystallization efficiency of the 15 mm pile length drainage pipe reached 10 – 60 % at all three flow rates, which was consistent with the research results of Liu [28]. The results showed that the diameter and length of the pile had an important influence on the anticrystallization

efficiency of the flocked drainage pipe. The results of the numerical simulation indicated that the three-dimensional flow field in the flocked drainage pipe changed abruptly in the section containing fluff, and there was a region where the flow velocity increased and decreased locally. The decrease in the flow velocity near the bottom of the drainage pipe was greater than that in the nonflocked drainage pipe, and the increase in flow velocity near the top and downstream of the fluff was also greater than that in the nonflocked drainage pipe. This was consistent with the two-dimensional flow field distribution characteristics in flocked drainage pipe reported by Liu et al. [27].

The contact area of the fluff and groundwater varies with the length of the fluff. The crystals are formed by chemical reactions between cations and anions, and they easily crystallize in the groundwater during the groundwater flow. The flow rate of the groundwater in the drainage pipe varied, and the corresponding cross sections and flow rates were different. As a result, the total amount of crystals in contact also differed. When the flow velocity of the groundwater in the drainage pipe was low, the flow section in the drainage pipe was small, and the fluff was completely wrapped in crystals in a short time. When the fluff was long, the total amount of crystals was larger than that for short fluff because of the capillary effect of the groundwater. When the velocity of the groundwater in the drainage pipe was high, the cross section of the water passing through the drainage pipe was large, and the short fluff was completely submerged. As a result, it was in full contact with the crystals in the groundwater. Because of the limited length of the fluff, the crystals wrapped around it also were limited. Because the longer villi had 70 – 100 % of their length submerged in the water, the contact area with the crystals was greater.

4. CONCLUSIONS

According to our results, we proposed the following:

1. The crystallization of nonflocked drainage pipe increased linearly, and the maximum crystallization rate was 1.30 g/day; The crystallization of flocked drainage pipe changes step by step, the maximum stable adhesion amount was 18.13 g, and the maximum anti crystallization efficiency can reach 80 %; The flocked drainage pipe can preferentially select the villus with the length of 5 mm and 10 mm.
2. The flow velocity of nonflocked drainage pipe increases gradually along the flow direction of water in the pipe, with a maximum increase of 50 % (at the water outlet) and a maximum increase of 35 % (at the top of the pile); There was an area where the velocity tends to 0 near the upstream and downstream of the flocked drainage pipe along the water flow direction, which was also the area where the crystals are most likely to adhere.
3. The numerical simulation crystal gradually adheres to the bottom of the pipe wall along the water flow direction, and deposits most near the water outlet, which is very consistent with the field investigation. The numerical simulation can be used to predict the variation of tunnel drainage pipe crystallization plugging with time.
4. Indoor tests have verified the feasibility of anti-crystallization blocking technology of flocking drainage pipe. A large number of experimental studies are needed for flocked drainage pipe parameters such as flocking material, length, diameter, longitudinal spacing and circumferential spacing. These parameters are also the key technology of anti-crystallization blocking of flocking drainage pipe. In addition, the mechanism of anti-crystallization blocking of flocking drainage pipe needs to be deeply studied, the connection mechanism between macro and micro of anti-crystallization blocking of flocking drainage pipe is established, and the anti-crystallization blocking management model of flocking drainage pipe is established.

Acknowledgments

This research was financially supported by the Scientific Research Project of the Emei Hanyuan Expressway Project (Grant No. LH-HT-45), and the State Key Laboratory of Mountain Bridge and Tunnel Engineering (Grant No. SKLBT-2110) and the Sub Project of National Key R&D Plan (2021YFB2600103-01), the Cooperation between Chongqing University and the Institute of Chinese Academy of Sciences (HZ2021009), and Chongqing Postgraduate Joint Training base Construction Project (JDLHPYJD2021003).

REFERENCES

1. **Zhao, P., Guo, X.X., Ma, W.B.** Research and Application of Dredge Equipment for Drainage Pipeline in Railway Tunnel *Railway Engineering* 58 (01) 2018: pp. 30 – 32.66. https://doi.org/10.3969/j.issn.1003-1995.2018.01.07
2. **Zhang, X.F., Zhou, Y.F., Zhang, B., Zhou, Y.J., Liu, S.Y.** Investigation and Analysis on Crystallization of Tunnel Drainage Pipes in Chongqing *Advances in Materials Science and Engineering* 2018: pp. 1 – 6. https://doi.org/10.1155/2018/7042693
3. **Guo, X.X.** Crystallization Mechanism and Countermeasures of Drainage System for Railway Tunnel *China Railway Science* 41 (01) 2020: pp. 71 – 77. CNKI:SUN:ZGTK.0.2020-01-011
4. **Lei, L., Hua, Y.L., Li, G.P., Qi, J., Li, D.W.** Analysis and Treatment of Blind Pipe Blockage in Humaling Tunnel on Lanzhou-Chongqing Railway *Modern Tunneling Technology* 57 (06) 2020: pp. 149 – 153. https://doi.org/10.13807/j.cnki.mtt.2020.06.020
5. **Wu, Y.Z., Li, G.P., Jia, Q.Q., Qi, H.Y., Li, D.W.** Study on Characteristics and Sources of Crystal Components of Leakage Water in the Loess Tunnel *Modern Tunneling Technology* 57 (06) 2020: pp. 154 – 159. https://doi.org/10.13807/j.cnki.mtt.2020.06.021
6. **Ye, F., Tian, C.M., He, B., Zhao, M., Wang, J., Han, X.B., Han, X.** Experimental Study on Scaling and Cloggingin Drainage System of Tunnels under Construction *China Journal of Highway and Transport* 34 (03) 2020: pp. 159 – 170. https://doi.org/10.19721/j.cnki.1001-7372.2021.03.011
7. **Jiang, Y.J., Du, K., Tao, L., Zhao, J.M., Xiao, H.R.** Investigation and Discussion on Blocking Mechanism of

Drainage System in Karst Tunnels *Railway Standard Design* 63 (07) 2019: pp. 131 – 135. https://doi.org/10.13238/j.issn.1004-2954.201804130001

8. **Tian, C.M., Ye, F., Song, G.F., Wang, Q.L., Zhao, M., He, B., Wang, J., Han, X,B.** Discussion on Mechanism of Crystal Blockage of Tunnel Drainage System and Preventive Countermeasures *Modern Tunneling Technology* 57 (05) 2020: pp. 66 – 76. https://doi.org/10.13807/j.cnki.mtt.2020.05.008
9. **Xiang, K., Zhou, J., Zhang, X.F., Huang, C., Song, L., Liu, S.Y.** Experimental Study on Crystallization Rule of Tunnel Drainpipe in Alkaline Environment *Tunnel Construction* 39 (S2) 2019: pp. 207 – 212. https://doi.org/10.3973/j.issn.2096-4498.2019.S2.027
10. **Zhou, Y.F., Zhang, X.F., Wei, L.W., Liu, S.Y., Zhang, B., Zhou, C.** Experimental Study on Prevention of Calcium Carbonate Crystallizing in Drainage Pipe of Tunnel Engineering *Advances in Civil Engineering* 2018 (04) 2018: pp. 1 – 11. https://doi.org/10.1155/2018/9430517
11. **Jiang, Y.J., Du, K., Liao, J.Y., Chen, X., Xiao, H.R.** Experimental Research on Maintainability of Drainage Facilities in Lining Construction Joints of Karst Tunnel *Railway Standard Design* 63 (11) 2019: pp. 91 – 96. https://doi.org/10.13238/j.issn.1004-2954.201901280001
12. **Ye, F., Tian, C.M., Zhao, M., He, B., Wang, J., Han, X.** The Disease of Scaling and Cloging in the Drainage Pipes of a Tunnel under Construction in Yunnan *China Civil Engineering Journal* 53 (S1) 2020: pp. 336 – 341. https://doi.org/10.15951/j.tmgcxb.2020.s1.053
13. **Su, Y.L., Yang, H.R., Shi, W.X., Guo, H.X., Zhao, Y., Wang, D.J.** Crystallization and Morphological Control of Calcium Carbonate by Functionalized Triblock Copolymers *Colloids and Surfaces A: Physicochemical and Engineering Aspects* 355 (1) 2009: pp. 158 – 162. https://doi.org/10.1016/j.colsurfa.2009.12.002
14. **Kirboga, S., Oner, M., Akyol, E.** The Effect of Ultrasonication on Calcium Carbonate Crystallization in the Presence of Biopolymer *Journal of Crystal Growth* 401 2014: pp. 266 – 270. https://doi.org/10.1016/j.jcrysgro.2013.11.048
15. **Su, M., Han, J., Li, Y.H., Chen, J.X., Zhao, Y.Y., Chadwick, K.** Ultrasonic Crystallization of Calcium Carbonate in Presence of Seawater Ions *Desalination* 369 2015: pp. 85 – 90. https://doi.org/10.1016/j.desal.2015.05.001
16. **Zhang, A.P., Feng, Z., Ding, Q., Xu, Z.M.** Simulation Study on influential of Ultrasonic Cavitation on Fouling Deposition Characteristic *CIESC Journal* 68 (S1) 2017: pp. 184 – 190. http://en.cnki.com.cn/Article_en/CJFDTOTAL-HGSZ2017S1026.htm
17. **Ge, H.H., Wei, C.J., Gong, X.M., Xu, X.M., Tao, J.T., Yao, X.P.** Effect of Electromagnetic Treatment on Sedimentation and Adhesion Behavior of Calcium Carbonate Particles Formed in Aqueous Solution *Acta Chimica Sinica* 69 (19) 2011: pp. 2313 – 2318. https://doi.org/10.1186/1752-153X-5-62
18. **Peng, C., Liang, Z., He, H.G., Zhang, L.F.** Influence of Magnetic Shielding Effect on Magnetic Descaling Results *Industrial Water Treatment* 35 (4) 2015: pp. 65 – 67. https://doi.org/10.11894/1005-829x.2015.35(4).065
19. **Wang, Y.F., Hou, F., Xu, H., Xia, X.M., Zeng, B.** Antiscaling Property Investigation on Electroless Ni-W-P Composite Coating *Chemical Industry and Engineering Progress* 30 (11) 2011: pp. 2558 – 2562. https://doi.org/10.1016/j.preteyeres.2010.11.001
20. **Cheng, Y.H., Zhang, S.J., Peng, Y.X., Zhu, Z.C., Cheng, L.** Fouling Characteristics on Amorphous Deposit Surface of Heat Exchangers *Journal of Engineering Thermophysics* 33 (5) 2012: pp. 828 – 830. http://qikan.cqvip.com/Qikan/Article/Detail?id=41729113
21. **Yong, F., Fu, C.Q., Luo, X.L., Wang, Z., Yao, J.L., Zheng, X.F.** Structure and Scaling Prevention Properties of Electroless Ni-Mo-P Alloy Coatings *Surface Technology* 44 (12) 2015: pp. 98 – 103. https://doi.org/10.16490/j.cnki.issn.1001-3660.2015.12.016
22. **Menzri, R., Ghizellaoui, S., Tlili, M.** Calcium Carbonate Inhibition by Green Inhibitors: Thiamine and Pyridoxine *Desalination* 404 2017: pp. 147 – 154. https://doi.org/10.1016/j.desal.2016.11.005
23. **Hong, Y.W., Qian, X.Q., Li, J.H., Yang, H.W., Zhang, P.** On Scavenging Performances of Cleaning Solvents for the Clogging in the Drainage System of Karst Tunnels *Modern Tunneling Technology* 57 (06) 2020: pp. 160 – 170. https://doi.org/10.13807/j.cnki.mtt.2020.06.022
24. **Liu, S.Y., Gao, F., Zhang, X.F., Han, F.L., Zhou, Y.F., Xiang, K., Xiao, D.J.** Experimental Study on Anti-Crystallization Law of Tunnel Transverse Flocking Drainpipe at Different Velocities *Asia-Pacific Journal of Chemical Engineering* 2020 (10) 2020: pp. 1 – 9. https://doi.org/10.1002/apj.2470
25. **Song, H.R., Huang, S.Y.** Crystallized Precipitation of Carbonate *Carsologica Sinica* 02 1990: pp. 3 – 16. http://www.cnki.com.cn/Article/CJFDTotal-ZGYR199002000.htm
26. **Feng, R.S., Zhou, J., Xiao, D.J., Chen, X.G., Li, H.M., Zhang, X.F.** Laboratory Experimental Study on Crystal Growth of Tunnel Drainage Pipe in High Temperature Area *Highway* 66 (09) 2021: pp. 398 – 402. http://qikan.cqvip.com/Qikan/Article/Detail?id=7105722168
27. **Liu, S.Y., Zhang, X.F., Gao, F., Wei, L.W., Liu, Q., Lü, H.Y., Wang, B.** Two-dimensional Flow Field Distribution Characteristics of Flocking Drainage Pipes in Tunnel *Open Physics* 18 (1) 2020: pp. 139 – 148. https://doi.org/10.1515/phys-2020-0013
28. **Liu, S.Y., Gao, F., Zhou, Y.F., Liu, Q., Lü, H.Y., Wang, B., Xiang, K., Xiao, D.J.** Effect of Fuzz Length on the Prevention of Crystallization of Tunnel Flocked Drainpipes *Science Technology and Engineering* 19 (9) 2019: pp. 234 – 239. https://doi.org/10.3969/j.issn.1671-1815.2019.09.037